

## 高磷诱导下肢血管平滑肌细胞成骨分化关键差异表达基因 筛选及验证

倪英群<sup>1,2,3</sup>, 杨 矛<sup>1</sup>, 杨 迪<sup>1</sup>, 郭呈林<sup>1</sup>, 朱文君<sup>4</sup>, 俞雅琴<sup>4</sup>, 卢 芹<sup>4</sup>, 骆金芝<sup>4</sup>, 吴春琴<sup>4</sup>, 方朝晖<sup>1,2,3</sup>

(1. 安徽中医药大学第一附属医院内分泌科, 安徽 合肥 230031; 2. 安徽省中医药科学院中医药防治糖尿病研究所, 安徽 合肥 230031; 3. 安徽中医药大学新安医学教育部重点实验室, 安徽 合肥 230038; 4. 安徽中医药大学研究生院, 安徽 合肥 230038)

**[摘要]** **目的:** 采用mRNA高通量测序技术筛选高磷诱导下肢血管平滑肌细胞(VSMCs)钙化差异表达基因(DEGs), 分析VSMCs钙化的关键基因及信号通路。**方法:** 将人VSMCs分为对照组和模型组, 模型组细胞中加入高磷培养基, 对照组细胞采用含10%胎牛血清的DMEM培养基于相同条件下培养。调整2组稳定转染VSMCs的状态, 培养12 d, 倒置显微镜下观察细胞形态表现并拍照。采用Hisat2软件筛选DEGs, 采用Stringtie软件从生物过程(BP)、分子功能(MF)和细胞成分(CC)3个方面进行基因本体论(GO)功能和京都基因与基因组百科全书(KEGG)信号通路富集分析。Von Kossa染色法观察各组细胞钙化情况, 实时荧光定量PCR(RT-qPCR)法检测2组细胞中碱性磷酸酶(ALP)、骨形态发生蛋白2(BMP2)、 $\alpha$ -平滑肌肌动蛋白( $\alpha$ -SMA)、肿瘤蛋白53(Tp53)、谷胱甘肽过氧化物酶4(GPX4)、铁蛋白轻链1(Ftl1)和糖基磷脂酰肌醇特异性磷脂酶D1(GPLD1)mRNA表达水平。**结果:** 与对照组比较, 模型组共2524个DEGs, 其中1368个DEGs表达上调, 1156个DEGs表达下调; 2组细胞DEGs聚类分离明显。GO功能和KEGG信号通路富集分析表达上调的DEGs主要参与微管细胞骨架组织的调节、细胞极性、蛋白质定位和细胞周期调控等BP, 构建细胞膜部分、微管组织、染色体和着丝粒区等CC, 发挥与磷脂酰肌醇磷酸盐、Rho鸟苷酸三磷酸酶(GTPase)蛋白结合、参与跨膜转运和调节蛋白激酶活性等MF; 表达下调的DEGs主要参与细胞质翻译、蛋白质膜定位、mRNA代谢和蛋白质内质网定位等BP, 构建核糖体亚单位、细胞膜和自噬体等CC, 发挥与单链DNA、核糖核蛋白复合物、生长因子结合、调节蛋白激酶活性和催化作用等MF。差异表达上调的基因富集7条信号通路, 其中最为显著的是糖基磷脂酰肌醇(GPI)锚定的生物合成; 差异表达下调的基因富集18条信号通路, 其中最为显著的是铁死亡。RT-qPCR法, 与对照组比较, 模型组细胞中GPX4、Ftl1和Tp53 mRNA表达水平明显降低( $P<0.01$ ), GPLD1 mRNA表达水平明显升高( $P<0.01$ ); 与对照组比较, 模型组细胞中 $\alpha$ -SMA mRNA表达水平明显降低( $P<0.01$ ), ALP和BMP2 mRNA表达水平明显升高( $P<0.01$ )。**结论:** 钙化的VSMCs与正常细胞存在DEGs, 铁死亡和GPI锚定的生物合成信号途径是高磷诱导下肢VSMCs钙化的关键信号通路, 主要由GPX4、Ftl1、Tp53和GPLD1共同介导完成。

**[关键词]** 血管平滑肌细胞; 成骨分化; 细胞钙化; mRNA测序; 铁死亡

**[中图分类号]** Q254 **[文献标志码]** A

**[收稿日期]** 2023-06-30

**[基金项目]** 国家自然科学基金项目(82274468); 安徽省教育厅高校优秀人才支持计划项目(gxyqZD2021114); 安徽中医药大学新安医学教育部重点实验室开放项目(2022XAYX06); 安徽中医药大学临床科研项目(2021yfyc07)

**[作者简介]** 倪英群(1981—), 女, 安徽省芜湖市人, 副主任医师, 医学博士, 主要从事中医药防治代谢内分泌疾病方面的研究。

**[通信作者]** 倪英群, 副主任医师, 硕士研究生导师(E-mail: Jessica8163@126.com)

## Screening of key differentially expressed genes involved in osteogenic differentiation of lower limb vascular smooth muscle cells and validation

NI Yingqun<sup>1,2,3</sup>, YANG Mao<sup>1</sup>, YANG Di<sup>1</sup>, GUO Chenglin<sup>1</sup>, ZHU Wenjun<sup>4</sup>, YU Yaqin<sup>4</sup>, LU Qin<sup>4</sup>,  
LUO Jinzhi<sup>4</sup>, WU Chunqin<sup>4</sup>, FANG Zhaohui<sup>1,2,3</sup>

(1. Department of Endocrinology, First Affiliated Hospital, Anhui University of Chinese Medicine, Hefei 230031, China; 2. Institute of Traditional Chinese Medicine for Prevention and Treatment of Diabetes, Anhui Academy of Chinese Medicine, Hefei 230031, China; 3. Key Laboratory of Xin An Medicine, Ministry of Education, Anhui University of Chinese Medicine, Hefei 230038, China; 4. Graduate School, Anhui University of Chinese Medicine, Hefei 230038, China)

**ABSTRACT Objective:** To screen the differentially expressed genes (DEGs) under high phosphate-induced calcification in the vascular smooth muscle cells (VSMCs) by mRNA high-throughput sequencing technology, and to analyze the key genes and signaling pathways involved in the VSMCs calcification. **Methods:** The human VSMCs were divided into control group and model group. The cells in model group was exposed to the high-phosphate medium, while the cells in control group were cultured in DMEM supplemented with 10% fetal bovine serum under the same conditions. The VSMCs in two groups, stably transfected, were cultured for 12 d. The morphology of the cells in two groups were observed and photographed under inverted microscope. The DEGs were selected by Hisat2 software, and Gene Ontology (GO) functional and Kyoto Encyclopedia of Genes and Genomes (KEGG) signaling pathway enrichment analysis were performed by Stringtie software from three aspects, such as biological processes (BP), molecular functions (MF), and cellular components (CC). The calcification of the cells in two groups was observed by Von Kossa staining method. Real-time fluorescence quantitative PCR (RT-qPCR) method was used to analyze the expression levels of alkaline phosphatase (ALP), bone morphogenetic protein 2 (BMP2), alpha-smooth muscle actin ( $\alpha$ -SMA), tumor protein 53 (Tp53), glutathione peroxidase 4 (GPX4), ferritin light chain 1 (Ftl1), and glycosylphosphatidylinositol-specific phospholipase D1 (GPLD1) mRNA in the cells in two groups. **Results:** Compared with control group, there were 2 524 DEGs in the cells in model group, and there were 1 368 upregulated DEGs and 1 156 downregulated DEGs. Clustering of DEGs between the cells in two groups was distinct. The GO functional and KEGG pathway enrichment analysis results showed that the upregulated DEGs were primarily involved in regulating the microtubule cytoskeleton, cell polarity, protein localization, and cell cycle regulation among BPs; in constructing cell membrane, microtubule organization, chromosomes, and kinetochore among CCs; and functioning in phosphatidylinositol phosphate, Rho GTPase protein binding, transmembrane transport, and protein kinase regulatory activity among MFs. Downregulated DEGs were mainly involved in cytoplasmic translation, protein membrane localization, mRNA metabolism, and protein endoplasmic reticulum localization among BPs; in forming ribosome subunits, cell membrane, and autophagy among CCs; and functioning in single-stranded DNA, ribonucleoprotein complex, growth factor binding, regulating protein kinase activity, and catalytic activity among MFs. Seven signaling pathways were significantly enriched in upregulated genes, most notably in the biosynthesis of glycosylphosphatidylinositol (GPI) anchors; whereas 18 signaling pathways were significantly enriched in the downregulated genes, most notably in ferroptosis. The RT-qPCR results showed that compared with control group, the expression levels of GPX4, Ftl1, and Tp53 mRNA in the cells in model group were significantly

decreased ( $P < 0.01$ ), while the expression level of GPLD1 mRNA was significantly increased ( $P < 0.01$ ); compared with control group, the expression level of  $\alpha$ -SMA mRNA in the cells in model group was significantly decreased ( $P < 0.01$ ), and the expression levels of ALP and BMP2 mRNA were significantly increased ( $P < 0.01$ ). **Conclusion:** The VSMCs underwent calcification and normal cells exhibit the DEGs. The key signaling pathways in the calcification induced by high phosphate in the VSMCs include ferroptosis and GPI anchor biosynthesis, mediated primarily through GPX4, Ftl1, Tp53, and GPLD1.

**KEYWORDS** Vascular smooth muscle cell; Osteogenic differentiation; Cell calcification; mRNA sequencing; Ferroptosis

血管钙化 (vascular calcification, VC) 是 2 型糖尿病 (type 2 diabetes mellitus, T2DM) 的重要危险因素, 其细胞学基础是血管平滑肌细胞 (vascular smooth muscle cells, VSMCs) 的成骨样分化。与正常人群比较, T2DM 患者的 VC 患病率明显升高<sup>[1-3]</sup>。与 T2DM 有关的 VC 在线粒体功能障碍<sup>[4]</sup>、慢性炎症<sup>[5]</sup> 和自噬<sup>[6]</sup> 等方面的研究有新的进展, 但其研究方向多集中于心血管动脉粥样硬化<sup>[7]</sup> 和慢性肾病<sup>[8]</sup> 等方面, 糖尿病下肢 VC 的研究较少。临床针对糖尿病下肢 VC 的治疗较为困难, 尚无特效药物, 主要以预防为主。因此, 探讨糖尿病下肢 VC 的发病机制有助于临床精准治疗, 对提高患者生存质量及预后具有重要意义。目前, 糖尿病下肢 VC 具体发病机制尚不明确。随着测序技术的发展, 转录组测序 (RNA sequencing, RNA-Seq) 技术和生物信息学分析在医学及药学领域中得到广泛应用, 可辅助相关医药学研究。本研究基于 RNA-Seq 技术筛选并验证高磷诱导下肢 VSMCs 钙化中差异表达基因 (differentially expressed genes, DEGs), 分析关键差异基因及信号通路, 为糖尿病 VC 发病机制的研究提供参考。

## 1 材料与方法

**1.1 细胞、主要试剂和仪器** 人 VSMCs (中国科学院细胞库)。总 RNA 文库制备相关试剂盒 (美国因美纳公司), 核酸片段筛选试剂盒 (美国贝克曼库尔公司), SuperScript IV 反转录酶 (美国赛默飞公司), 铁蛋白轻链 1 (ferritin light polypeptide-1, Ftl1)、肿瘤蛋白 53 (tumor protein 53, Tp53)、糖基化磷脂酰肌醇特异性磷脂酶 D1 (glycosylphosphatidylinositol specific phospholipase D1, GPLD1) 和谷胱甘肽过氧化酶 4 (glutathione peroxidase 4, GPX4) 试剂盒 (英国 Abcam 公司), 4% 多聚甲醛 (上海碧云天生物技术股份有限公司), Von Kossa 银

溶液 (上海康朗生物科技有限公司)。超速冷冻离心机 (湖南湘仪公司), 酶标仪 (美国 BioTek 公司), 荧光显微镜 (日本奥林巴斯公司), 紫外分光光度计 (型号: NanoDrop 2000)、荧光定量仪 (型号: Invitrogen Qubit 3.0)、PCR 扩增仪 (型号: ABI 2720 Thermal Cycler) 和 Ambion 磁性底座 (美国赛默飞公司), 离心机 (型号: Eppendorf 5810R, 德国艾本德公司), 核酸电泳分析仪 (型号: Agilent 2100 bioanalyzer, 美国安捷伦公司), 基因测序仪 (型号: Illumina novaseq 6000, 美国因美纳公司), 实时荧光定量 PCR (real-time fluorescence quantitative PCR, RT-qPCR) 仪 (瑞士罗氏公司)。

**1.2 细胞分组和造模** 将人 VSMCs 分为对照组和模型组。根据参考文献 [9-10] 中方法建立模型。模型组细胞中加入高磷培养基 (含  $10 \text{ mmol} \cdot \text{L}^{-1}$   $\beta$ -甘油磷酸盐、 $50 \text{ g} \cdot \text{L}^{-1}$  维生素 C 和  $1 \times 10^{-7} \text{ mol} \cdot \text{L}^{-1}$  胰岛素的高糖 DMEM 培养基) 诱导细胞钙化, 于  $37 \text{ }^\circ\text{C}$ 、 $5\% \text{ CO}_2$  条件下进行培养。为模拟 T2DM 患者体内环境, 在钙化诱导的平滑肌细胞中加入  $50 \text{ mg} \cdot \text{L}^{-1}$  氧化型低密度脂蛋白 (oxidized low density lipoprotein, ox-LDL) 和  $10 \text{ } \mu\text{mol} \cdot \text{L}^{-1}$  羧甲基赖氨酸 (N $\epsilon$ -carboxymethyl-lysine, CML)。对照组细胞采用含 10% 胎牛血清的 DMEM 培养基于模型组相同条件下培养。调整 2 组稳定转染 VSMCs 的状态, 培养 12 d, 倒置显微镜下观察细胞形态表现并拍照。由合肥麟美生物科技有限公司提供稳定转染细胞转录组测序。

**1.3 DEGs 筛选和基因本体论 (Gene Ontology, GO) 功能及京都基因与基因组百科全书 (Kyoto Encyclopedia of Genes and Genomes, KEGG) 信号通路富集分析** 采用 Hisat2 软件筛选 DEGs, 采用 Stringtie 软件从生物过程 (biological process, BP)、分子功能 (molecular function, MF) 和细胞成分 (cellular component, CC) 3 个方面进行 GO 功能及

KEGG 信号通路富集分析。采用微生信在线作图 (<http://www.bioinformatics.com.cn/>) 进行可视化处理, 绘制图像。

#### 1.4 Von Kossa 染色法观察各组细胞钙化情况

采用 4% 多聚甲醛固定细胞, 加入 Von Kossa 银溶液, 强光照射 15~60 min, 蒸馏水洗涤 1 min, 加入硫代硫酸钠溶液处理 2 min。Van Gieson 染色液复染细胞, 于电镜下观察并拍照。

**1.5 RT-qPCR 法检测 2 组细胞中碱性磷酸酶 (alkaline phosphatase, ALP)、骨形态发生蛋白 2 (bone morphogenetic protein 2, BMP2)、 $\alpha$ -平滑肌肌动蛋白 (alpha-smooth muscle actin,  $\alpha$ -SMA)、Tp53、GPX4、Ftl1 和 GPLD1 mRNA 表达水平** 采用 TRIzol 法提取细胞总 RNA, 反转录获取 cDNA, 进行 PCR 扩增。反应条件: 95 °C 预变性 3 min, 扩增 95 °C、15 s, 60 °C、30 s, 共 40 个循环。引物序列见表 1。采用  $2^{-\Delta\Delta Ct}$  法计算目的基因表达水平。

表 1 引物序列  
Tab. 1 Primer sequences

Gene		Primer sequence(5'-3')
ALP	Forward	GTGGTATTGTAGGTGCTGTGGTC
	Reverse	ACGGTGTCTAGCCTTCTGG
BMP2	Forward	GTTCTGTCCCTACTGATGAGTTTCT
	Reverse	CTGGCTGTGGCAGGCTTTAT'
$\alpha$ -SMA	Forward	GGGCATCCACGAAACCACCT
	Reverse	GAGCCGCCGATCCAGACAGA
TP53	Forward	GCCATCTACAAGAAGTCACAACAC
	Reverse	TGTCGTCCAGATACTCAGCATACT
GPX4	Forward	CAATGAGGCAAAACCGACGTA
	Reverse	CCTCCCGAACTGGTTGCAAG
Ftl1	Forward	CAGCCTGGTCAATTTGTACCT
	Reverse	GCCAATTCGCGGAAGAAGTG
GPLD1	Forward	GGTGGGCTCGAGCAT
	Reverse	GCACCTTTGTAGGTGAGCAG

**1.6 统计学分析** 采用 SPSS 23.0 统计软件进行统计学分析。2 组细胞中 ALP、BMP2、 $\alpha$ -SMA、Tp53、GPX4、Ftl1 和 GPLD1 mRNA 表达水平符合正态分布, 以  $\bar{x} \pm s$  表示, 2 组间样本均数比较采用两独立样本 *t* 检验。以  $P < 0.05$  为差异有统计学意义。

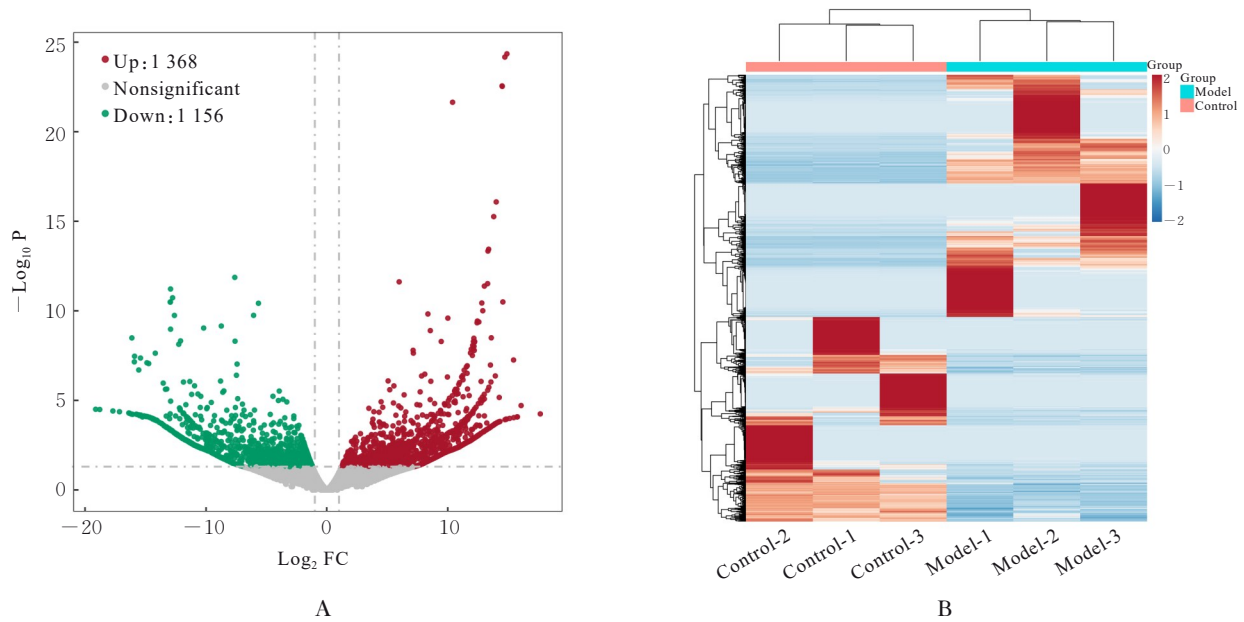
## 2 结果

**2.1 2 组细胞 DEGs 和聚类分析** 与对照组比较, 模型组细胞共有 2 524 个 DEGs, 其中 1 368 个 DEGs 表达上调, 1 156 个 DEGs 表达下调。将 DEGs 进行聚类分析, 结果显示: 2 组细胞 DEGs 聚类分离明显。见图 1。

**2.2 GO 功能和 KEGG 信号通路富集分析** 表达上调的 DEGs 主要参与微管细胞骨架组织的调节、细胞极性、蛋白质定位和细胞周期调控等 BP, 构建细胞膜部分、微管组织、染色体和着丝粒区等 CC, 发挥与磷脂酰肌醇磷酸盐、Rho 鸟苷酸三磷酸酶 (guanosine triphosphatase, GTPase) 蛋白结合、参与跨膜转运和调节蛋白激酶活性等 MF; 表达下调的 DEGs 主要参与细胞质翻译、蛋白质膜定位、mRNA 代谢和蛋白质内质网定位等 BP, 构建核糖体亚单位、细胞膜和自噬体等 CC, 发挥与单链 DNA、核糖核蛋白复合物、生长因子结合、调节蛋白激酶活性和催化作用等 MF。见图 2。差异表达上调的基因富集 7 条信号通路, 其中最为显著的是糖基磷脂酰肌醇 (glycosylphosphatidylinositol, GPI) 锚定的生物合成; 表达下调的 DEGs 富集 18 条信号通路, 其中最为显著的是铁死亡。GPI 锚定的生物合成信号通路中共 3 个上调的 DEGs, 分别为磷脂酰肌醇聚糖锚定生物合成 V (phosphatidylinositol glycan anchor biosynthesis class V, Pigtv)、GPLD1 和磷脂酰肌醇聚糖锚定生物合成 C (phosphatidylinositol glycan anchor biosynthesis class C, Pigtc)。铁死亡信号通路共 8 个下调的 DEGs, 分别为 LOC100360087、AABR07004746.1、Ftl1、Rho 家族相互作用细胞极化调节因子 2 (Rho family interacting cell polarization regulator 2, Ripor2)、精胺/精胺 N1-乙酰基转移酶 (spermidine/spermine N1-acetyltransferase 1, Sat1)、GPX4、Tp53 和电压依赖性阴离子通道 2 (voltage-dependent anion channel 2, Vdac2)。见图 3。

**2.3 2 组细胞形态表现** Von Kossa 染色法观察可见对照组细胞生长正常, 细胞密度高, 细胞形态正常, 未见明显的钙化细胞; 模型组细胞生长缓慢, 细胞密度较低, 细胞形态发生变化, 可见明显的钙化细胞黑褐色位点。见图 4。

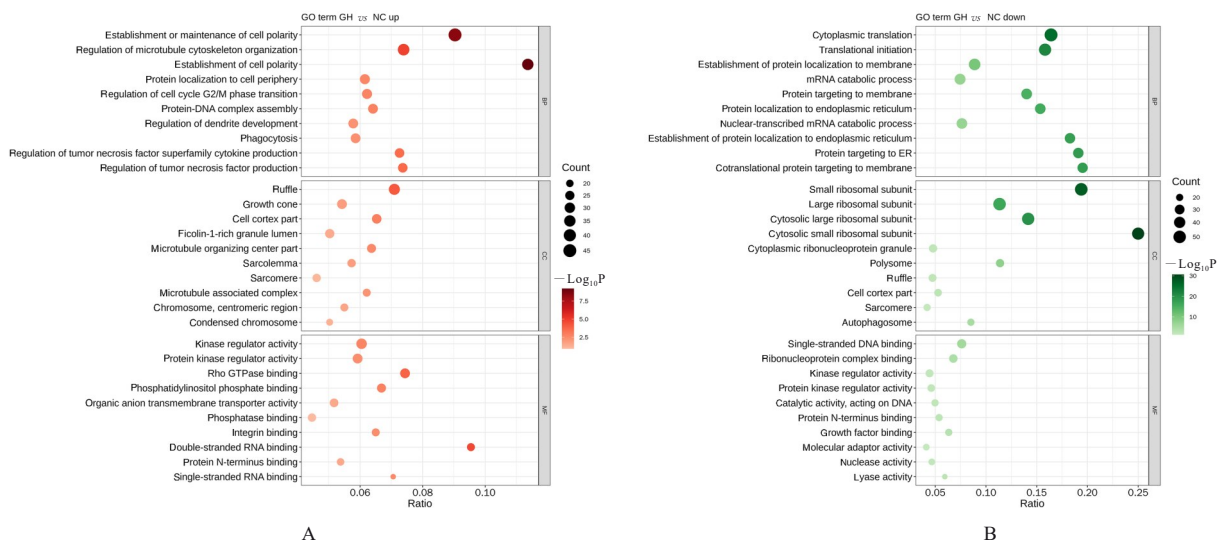
**2.4 2 组细胞中  $\alpha$ -SMA、ALP 和 BMP2 mRNA 表达水平** 与对照组比较, 模型组细胞中  $\alpha$ -SMA



A: Volcano map of DEGs (Red and blue dots were genes with significant differential expression, gray dots were genes without significant differential expression); B: Cluster analysis chart (Red represented high expression genes and blue represents low expression genes).

图1 2组细胞DEGs火山图和聚类分析图

Fig. 1 Volcano map and cluster analysis chart of DEGs in cells in two groups



A: Upregulated mRNA; B: Downregulated mRNA.

图2 DEGs的GO功能富集分析

Fig. 2 GO functional enrichment analysis on DEGs

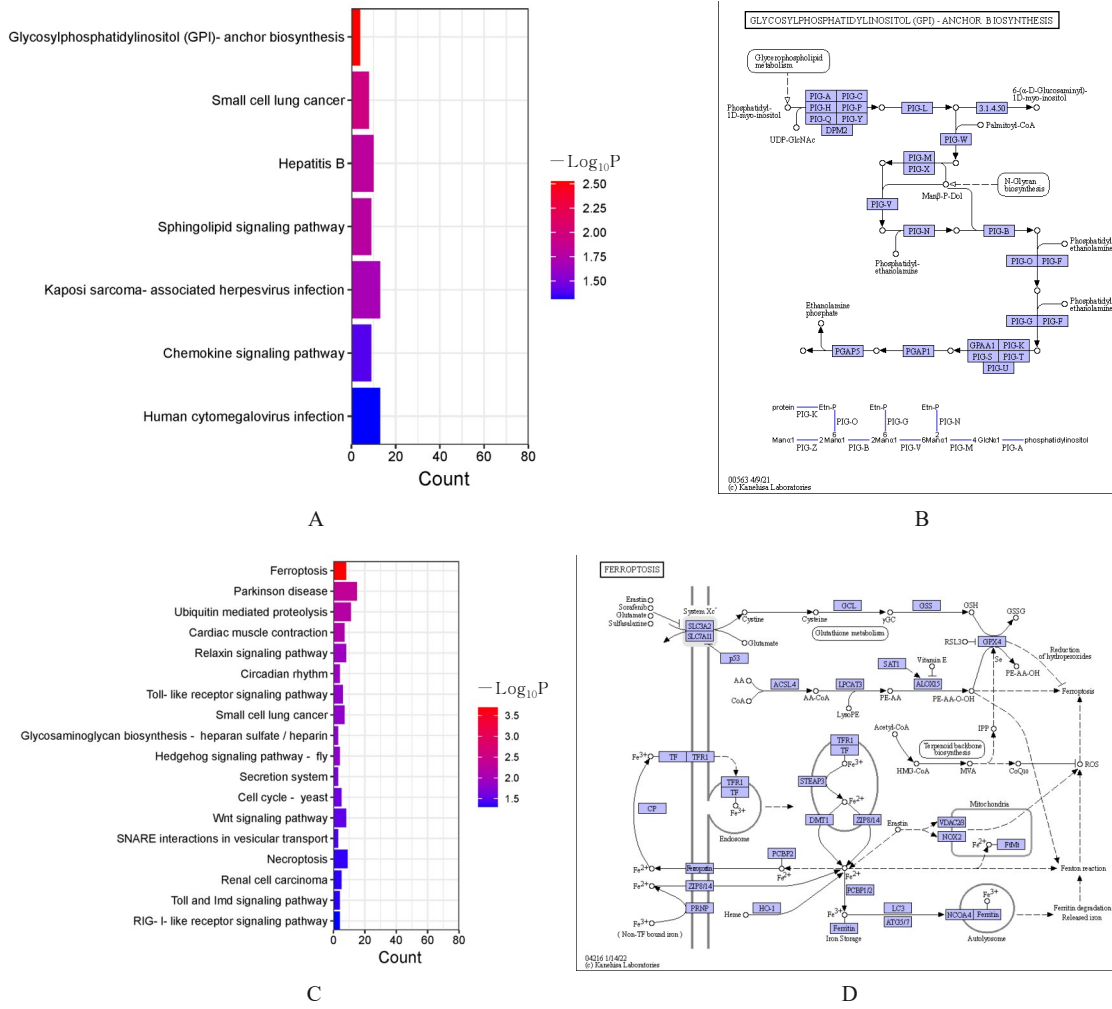
mRNA 表达水平明显降低 ( $P < 0.01$ ), ALP 和 BMP2 mRNA 表达水平明显升高 ( $P < 0.01$ )。见表2。

**2.5 2组细胞中GPX4、Ftl1、Tp53和GPLD1 mRNA 表达水平** 与对照组比较, 模型组细胞中GPX4、Ftl1 和 Tp53 mRNA 表达水平明显降低 ( $P < 0.01$ ), GPLD1 mRNA 表达水平明显升高 ( $P <$

$0.01$ )。见表3。

### 3 讨论

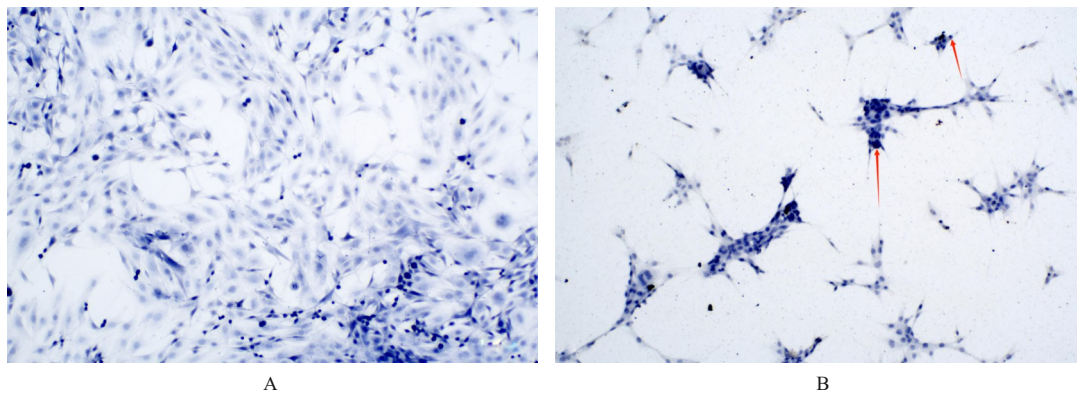
目前全球糖尿病患病率逐年升高, 预计至2030年约有5.784亿人患有糖尿病<sup>[11]</sup>。VC是糖尿病患者常见的并发症, 也是糖尿病患者疾病恶化、心血管疾病发病率升高和患者死亡的危险因素。



A: KEGG enrichment map of upregulated DEGs (Red to blue indicated a gradual decrease in differences, and red was most significant); B: Biosynthetic signaling pathway map anchored by GPI; C: KEGG enrichment map of downregulated DEGs; D: Signaling pathway map of ferroptosis (Red to blue indicated a gradual decrease in differences, and red was most significant).

图3 DEGs的KEGG信号通路富集分析

Fig. 3 KEGG signaling pathway enrichment analysis on DEGs



Red arrows indicated calcified cells. A:Control group;B:Model group.

图4 Von Kossa染色法观察2组细胞形态表现(×100)

Fig. 4 Morphology of cells in two groups observed by Von Kossa staining method(×100)

表2 2组细胞中 $\alpha$ -SMA、ALP和BMP2 mRNA表达水平  
Tab. 2 Expression levels of  $\alpha$ -SMA, ALP, and BMP2 mRNA in cells in two groups ( $n=3, \bar{x} \pm s$ )

Group	$\alpha$ -SMA	ALP	BMP2
Control	1.00 $\pm$ 0.02	1.00 $\pm$ 0.02	1.00 $\pm$ 0.01
Model	0.41 $\pm$ 0.01*	5.11 $\pm$ 0.11*	5.62 $\pm$ 0.03*

\* $P < 0.01$  vs control group.

表3 2组细胞中GPLD1、GPX4、Ftl1和Tp53 mRNA表达水平

Tab. 3 Expression levels of GPLD1, GPX4, Ftl1, and Tp53 mRNA in cells in two groups ( $n=3, \bar{x} \pm s$ )

Group	GPLD1	GPX4	Ftl1	Tp53
Control	1.00 $\pm$ 0.03	1.00 $\pm$ 0.17	1.00 $\pm$ 0.12	1.00 $\pm$ 0.12
Model	2.24 $\pm$ 0.07*	0.53 $\pm$ 0.09*	0.36 $\pm$ 0.01*	0.41 $\pm$ 0.11*

\* $P < 0.01$  vs control group.

VSMCs是负责血管功能的主要细胞,在受到氧化应激和高葡萄糖水平等条件刺激时,分泌大量的ALP、 $\alpha$ -SMA和BMP2等骨相关蛋白,进而发生细胞表型转化,由原始的收缩表型转变为成骨细胞样表型<sup>[12]</sup>。重组BMP2增强了高钙和磷酸盐诱导的VSMCs钙化,同时失去收缩表型标记 $\alpha$ -SMA<sup>[12-13]</sup>。细胞通过产生局部的前钙化促进内侧钙化环境,为钙和磷酸盐提供成核位点沉淀及磷酸钙晶体生长。

为更好地从转录组学水平了解糖尿病下肢VC的发病机制,本研究采用高磷诱导人下肢VSMCs钙化, RNA-seq技术分析DEGs,结果显示:钙化细胞中共有2524个DEGs,其中1368个上调,1156个下调;对照组和模型组细胞DEGs聚类显著分离。DEGs通过参与微管细胞骨架组织的调节、蛋白质定位、细胞周期调控、mRNA代谢和蛋白质内质网定位等细胞BP影响细胞钙化的发生。KEGG信号通路富集分析结果显示:高磷诱导的下肢VSMCs中上调的DEGs主要富集于7条信号通路上,最显著的是GPI锚定的生物合成途径。GPLD1与多种慢性疾病的发生发展有关,可以裂解细胞膜上被GPI锚定的蛋白质,从而发挥生物学效应,如糖脂代谢调节和神经系统疾病调控等<sup>[14-16]</sup>。研究<sup>[17]</sup>显示:糖尿病模型大鼠血液中GPLD1水平显著高于正常组大鼠。GPLD1通过裂解GPI锚定细胞膜蛋白,上调巨噬细胞的细胞因子表达,影响糖尿病进程<sup>[18]</sup>。研究<sup>[19]</sup>显示:胰岛素可以抑制GPLD1的合成,降低血循环中GPLD1水平,改善大鼠血

糖。本研究结果显示:下调的DEGs主要富集于18条信号通路上,最为显著的是铁死亡途径。细胞中铁蛋白重链1(ferritin heavy polypeptide 1, Fth1)和Ftl1表达下调导致铁过载<sup>[20]</sup>。铁过载通过诱导细胞凋亡和铁死亡而促进内皮细胞钙化。铁螯合剂和铁死亡抑制剂可减轻铁过载引起的铁死亡及钙化<sup>[21]</sup>。在促成骨条件下,铁死亡诱导剂诱导谷胱甘肽(glutathione, GSH)消耗,促进VSMCs钙化,而N-乙酰半胱氨酸补充GSH,抑制VSMCs钙化。高钙和磷酸盐下调GPX4的表达,并降低谷胱甘肽过氧化物酶活性,促进VSMCs钙化<sup>[8]</sup>。

本研究结果显示:模型组细胞生长缓慢,有明显的钙化点,表明高磷诱导的VSMCs发生钙化。为进一步验证参与细胞钙化的关键分子,本研究在生物信息学分析结果的基础上对目标分子进行RT-qPCR法检测结果显示:与对照组比较,模型组细胞铁死亡通路的GPX4、Ftl1和Tp53 mRNA表达水平明显降低, GPI锚定的生物合成通路的GPLD1 mRNA表达水平明显升高,同时表型蛋白 $\alpha$ -SMA mRNA表达水平明显降低, ALP和BMP2 mRNA表达水平明显升高。提示高磷诱导的VSMCs钙化可能是由铁死亡和GPI锚定的生物合成途径共同介导完成的。

综上所述,钙化的VSMCs与正常细胞存在DEGs的基因,铁死亡和GPI锚定的生物合成信号途径是高磷诱导下肢VSMCs钙化的关键信号通路,主要由GPX4、Ftl1、Tp53和GPLD1共同介导完成。

#### 利益冲突声明:

所有作者声明不存在利益冲突。

#### 作者贡献声明:

倪英群参与论文选题、研究设计、论文撰写和审校,杨矛、杨迪和郭呈林参与统计学分析,朱文君、俞雅琴、卢芹、骆金芝和吴春琴参与数据采集及文献检索,方朝晖参与论文选题、研究设计和论文审校。

#### [参考文献]

- [1] ALMAN A C, MAAHS D M, REWERS M J, et al. Ideal cardiovascular health and the prevalence and progression of coronary artery calcification in adults with and without type 1 diabetes [J]. *Diabetes Care*, 2014, 37(2): 521-528.
- [2] BERRY C, TARDIF J C, BOURASSA M G. Coronary heart disease in patients with diabetes: part I:

- recent advances in prevention and noninvasive management[J]. *J Am Coll Cardiol*, 2007, 49(6): 631-642.
- [3] YAHAGI K, KOLODZIE F D, LUTTER C, et al. Pathology of human coronary and carotid artery atherosclerosis and vascular calcification in diabetes mellitus[J]. *Arterioscler Thromb Vasc Biol*, 2017, 37(2): 191-204.
- [4] WANG P W, PANG Q, ZHOU T, et al. Irisin alleviates vascular calcification by inhibiting VSMC osteoblastic transformation and mitochondria dysfunction via AMPK/Drp1 signaling pathway in chronic kidney disease[J]. *Atherosclerosis*, 2022, 346: 36-45.
- [5] SÁNCHEZ-DUFFHUES G, GARCÍA DE VINUESA A, VAN DE POL V, et al. Inflammation induces endothelial-to-mesenchymal transition and promotes vascular calcification through downregulation of BMPR2[J]. *J Pathol*, 2019, 247(3): 333-346.
- [6] LIU Q, LUO Y, ZHAO Y, et al. Nano-hydroxyapatite accelerates vascular calcification via lysosome impairment and autophagy dysfunction in smooth muscle cells[J]. *Bioact Mater*, 2021, 8: 478-493.
- [7] AHN B Y, JEONG Y, KIM S, et al. Cdon suppresses vascular smooth muscle calcification via repression of the Wnt/Runx2 Axis[J]. *Exp Mol Med*, 2023, 55(1): 120-131.
- [8] YE Y Z, CHEN A, LI L, et al. Repression of the antiporter SLC7A11/glutathione/glutathione peroxidase 4 axis drives ferroptosis of vascular smooth muscle cells to facilitate vascular calcification[J]. *Kidney Int*, 2022, 102(6): 1259-1275.
- [9] WANG Z Q, JIANG Y C, LIU N F, et al. Advanced glycation end-product N $\epsilon$ -carboxymethyl-Lysine accelerates progression of atherosclerotic calcification in diabetes[J]. *Atherosclerosis*, 2012, 221(2): 387-396.
- [10] 高敏, 陈天雷, 吴琳, 等. 吡格列酮通过 Wnt/ $\beta$ -catenin 信号通路减轻大鼠血管平滑肌细胞钙化[J]. *肾脏病与透析肾移植杂志*, 2016, 25(4): 340-346.
- [11] YAO H P, SUN Z, ZANG G Y, et al. Epidemiological research advances in vascular calcification in diabetes[J]. *J Diabetes Res*, 2021, 2021: 4461311.
- [12] VOELKL J, LANG F, ECKARDT K U, et al. Signaling pathways involved in vascular smooth muscle cell calcification during hyperphosphatemia[J]. *Cell Mol Life Sci*, 2019, 76(11): 2077-2091.
- [13] KONG Y L, LIANG Q C, CHEN Y T, et al. Hyaluronan negatively regulates vascular calcification involving BMP2 signaling[J]. *Lab Invest*, 2018, 98(10): 1320-1332.
- [14] MASUDA S, FUJISHIMA Y, MAEDA N, et al. Impact of glycosylphosphatidylinositol-specific phospholipase D on hepatic diacylglycerol accumulation, steatosis, and insulin resistance in diet-induced obesity[J]. *Am J Physiol Endocrinol Metab*, 2019, 316(2): E239-E250.
- [15] RAIKWAN N S, BOWEN-DEEG R F, DU X S, et al. Glycosylphosphatidylinositol-specific phospholipase D improves glucose tolerance[J]. *Metabolism*, 2010, 59(10): 1413-1420.
- [16] TORRETTA S, RAMPINO A, BASSO M, et al. NURR1 and ERR1 modulate the expression of genes of a DRD2 coexpression network enriched for schizophrenia risk[J]. *J Neurosci*, 2020, 40(4): 932-941.
- [17] ABDOLMALEKI F, HEIDARIANPOUR A. Endurance exercise training restores diabetes-induced alteration in circulating Glycosylphosphatidylinositol-specific phospholipase D levels in rats [J]. *Diabetol Metab Syndr*, 2020, 12: 43.
- [18] QIN W, LIANG Y Z, QIN B Y, et al. The clinical significance of glycoprotein phospholipase D levels in distinguishing early stage latent autoimmune diabetes in adults and type 2 diabetes[J]. *PLoS One*, 2016, 11(6): e0156959.
- [19] SCHOFIELD J N, STEPHENS J W, HUREL S J, et al. Insulin reduces serum glycosylphosphatidylinositol phospholipase D levels in human type I diabetic patients and streptozotocin diabetic rats [J]. *Mol Genet Metab*, 2002, 75(2): 154-161.
- [20] WANG K, CHEN X Z, WANG Y H, et al. Emerging roles of ferroptosis in cardiovascular diseases [J]. *Cell Death Discov*, 2022, 8(1): 394.
- [21] ZHAO L L, YANG N, SONG Y Q, et al. Effect of iron overload on endothelial cell calcification and its mechanism[J]. *Ann Transl Med*, 2021, 9(22): 1658.